A SIMPLE SCHEME FOR THE APPROXIMATION OF SELF-AVOIDING INEXTENSIBLE CURVES

SÖREN BARTELS, PHILIPP REITER, AND JOHANNES RIEGE

ABSTRACT. The discretization of a tangent-point potential with a C^1 conforming finite element method is investigated. Error bounds for the practical evaluation of the potential and its variation are derived. A numerical scheme for the minimization of a weighted sum of bending energy and potential is devised and tested numerically for open and closed curves.

1. INTRODUCTION

Simulating curves describing the bending behaviour of elastic rods is a challenging mathematical problem, cf. [DKS02, BGN12, Bar13, DLP14, PS15], which has applications in the modeling of cell filaments [MOSS15], textile fabrication processes [GM15], and the determination of equivalence classes of knots [GRvdM15]. A rigorous dimension reduction from three-dimensional elasticity shows that when large deformations occur, an inextensibility constraint has to be incorporated [MM03]. In the simplest setting the elastic bending energy is then given by

$$I_{\mathrm{bend}}(u) = \frac{1}{2}\int_I |u''(y)|^2 \,\mathrm{d}y, \quad |u'(y)|^2 = 1.$$

The constraint implies that the curve described by the function $u : I \to \mathbb{R}^3$ is parametrized by arc-length and $u''(y)$ is its curvature vector.
Stable and convergent finite element methods using piecewise cubic, C^1 conforming finite elements have been devised and analyzed in [Bar13]. The constraint is imposed at the nodes of the underlying partition and critical configurations for I_{bend} subject to clamped or periodic boundary conditions are obtained by approximating a solution $u : [0,T]\times I \to \mathbb{R}^3$ of the evolution determined by the gradient flow

$$(\partial_t u, v) = -\delta I_{\mathrm{bend}}(u)[v], \quad u(0) = u_0,$$

for a suitable scalar product $(\cdot,\cdot)$ on $H^2(I,\mathbb{R}^3)$, an initial curve $u_0 : I \to \mathbb{R}^3$, and curves $v : I \to \mathbb{R}^3$ satisfying corresponding homogeneous boundary conditions and the orthogonality relation

$$u'(t,y)\cdot v'(t,y) = 0$$

Date: October 6, 2016.

for all $y \in I$ and $t \in [0,T]$, which is the linearization of the inextensibility constraint about the curve u.

A natural requirement is to restrict the evolution or minimization to embedded curves $u : I \to \mathbb{R}^3$ and to determine isotopies from initial data, i.e., the topological equivalence class is preserved. Only few articles are available devising numerical schemes for this purpose, e.g., [Her12, Wal16]. One way to realize this is to include a potential that avoids non-injective curves. An outline on the discretization of several self-avoiding energies is provided in [Sch16]. One possible choice is a repulsive tangent-point potential proposed in [GM99] given for $q \geq 2$ by

$$\mathrm{TP}(u) = \frac{2^{-q}}{q} \int_I \int_I \frac{1}{\mathbf{r}^q\big(u(y),u(x)\big)} \,\mathrm{d}x\,\mathrm{d}y.$$

The potential takes values in $[0,\infty]$, see [SvdM12] and references therein, and is a knot energy for $q > 2$ in the sense that for a sequence of embedded curves $(u_k) \subset W^{2-1/q,q}(I,\mathbb{R}^3)$ converging pointwise to a nonembedded curve we have $\mathrm{TP}(u_k) \to \infty$, see [SSvdM13, Bla13, BR15]. The tangent-point radius $\mathbf{r}(u(y),u(x))$ is the radius of the circle that is tangent to u in the point $u(y)$ and which intersects with u in $u(x)$, i.e.,

$$\mathbf{r}\big(u(x),u(y)\big) = \frac{|u(y)-u(x)|^2}{2\,\mathrm{dist}(\ell(y),u(x))} = \frac{|u(y)-u(x)|}{2\sin(u'(y),u(y)-u(x))}$$

with the tangent line $\ell(y) = \{u(y) + \mu u'(y) : \mu \in \mathbb{R}\}$ and $\sin(a,b)$ denoting the sine of the angle between the vectors $a,b \in \mathbb{R}^3$, cf. Fig. 1(a). If $u(x) = u(y)$ then the radius vanishes which causes a singularity in the potential, cf. Fig. 1(b).

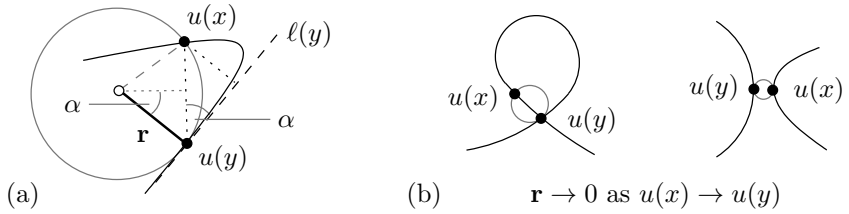

FIGURE 1. (a) Tangent-point function $\mathbf{r} = \mathbf{r}(u(y),u(x))$ for a curve u; (b) the radius $\mathbf{r}$ vanishes at self-intersections.

Using that $|\sin(a,b)| = |a \wedge b|/(|a||b|)$ and $|u'(y)| = 1$ we may write the radius $\mathbf{r}$ as

$$\mathbf{r}\big(u(x),u(y)\big) = \frac{1}{2}\frac{|u(y)-u(x)|^2}{|u'(y) \wedge [u(y)-u(x)]|}.$$

For $x \approx y$ we have that the inverse of the radius approximates the curvature $|u''(y)|/2$. This is our motivation to extract the singular diagonal from the

integral and to consider the approximation

$$\mathrm{TP}_\varepsilon(u) = \frac{1}{q}\int_I \int_{I_\varepsilon(y)} \frac{|u'(y) \wedge [u(y)-u(x)]|^q}{|u(y)-u(x)|^{2q}}\,\mathrm{d}x\,\mathrm{d}y,$$

where $I_\varepsilon(y) = I \setminus B_\varepsilon(y)$. We provide a rigorous justification of this simplification via an error estimate; for sufficiently regular curves u the approximation is linear in ε, in general, i.e., if $u \in H^2 \cap W^{2-1/q,q}$, $q < 4$, we have the approximation order $\mathcal{O}(\varepsilon^{2-q/2-\delta})$ for every $\delta \in (0, 2-q/2)$.

Based on the approximation of the tangent-point potential we devise discretizations of the potential and its variation. The resulting discrete operators allow us to define a semi-implicit scheme for approximating evolutions determined by the gradient flow of a weighted sum of bending energy and tangent-point potential, i.e., with a parameter $\varrho > 0$,

$$(\partial_t u, v) = -\delta\big(I_{\mathrm{bend}}(u) + \varrho \mathrm{TP}_\varepsilon(u)\big)[v],$$

within the class of arc-length parametrized curves. Crucial for good stability properties is a splitting of the variation of TP_ε into an antimonotone and remaining part, i.e., we define mappings $\mathcal{M}_\varepsilon$ and $\mathcal{A}_\varepsilon$ such that

$$\delta\mathrm{TP}_\varepsilon(u)[v] = \mathcal{M}_\varepsilon(u;u,v) + \mathcal{M}_\varepsilon(u;v,u) - 2\mathcal{A}_\varepsilon(u;u,v).$$

For fixed $\widetilde{u}$ in the first component the mappings

$$(v,w) \mapsto \mathcal{M}_\varepsilon(\widetilde{u};v,w), \quad (v,w) \mapsto \mathcal{A}_\varepsilon(\widetilde{u};v,w)$$

are bilinear forms with the properties that $\mathcal{A}_\varepsilon(\widetilde{u};\cdot,\cdot)$ is positive semi-definite while the quantity $\mathcal{M}_\varepsilon(\widetilde{u};\widetilde{u},\widetilde{u})$ is positive. Our semi-implicit time stepping scheme thus computes a sequence $(u^k)_{k=0,1,\dots}$ such that

$$\begin{aligned}\big(d_t u^k, v\big) + \big([u^k]'', v''\big) + \varrho\big[\mathcal{M}_\varepsilon(u^{k-1};u^k,v) + \mathcal{M}_\varepsilon(u^{k-1};v,u^k)\big]& \\ = 2\varrho\mathcal{A}_\varepsilon(u^{k-1};u^{k-1},v)&\end{aligned}$$

with the backward difference quotient $d_t u^k = (u^k - u^{k-1})/\tau$ and for all suitable test functions v that satisfy the orthogonality relation

$$[u^{k-1}]' \cdot v' = 0$$

in I. Motivated by the identity $u \cdot \partial_t u = 0$, the same condition is imposed on the discrete time-derivative, i.e.,

$$[u^{k-1}]' \cdot [d_t u^k]' = 0$$

in I. Every time step thus requires the solution of a well-posed, constrained, symmetric linear system of equations.

If the initial curve u^0 satisfies $|[u^0]'|^2 = 1$ then the orthogonality relation, the identity $u^k = u^{k-1} + \tau d_t u^k$, and an inductive argument lead to

$$|[u^k]'|^2 = |[u^{k-1}]'|^2 + \tau^2|[d_t u^k]'|^2 = \cdots = 1 + \tau^2 \sum_{\ell=1}^{k} |[d_t u^\ell]'|^2.$$

Because of the gradient flow dynamics and corresponding bounds on the time derivative we expect that the second term on the right-hand side is

of order $\mathcal{O}(\tau)$ up to negative powers of mesh-size related to the use of inverse estimates. Therefore no projection is needed to obtain curves that approximately satisfy the arc-length constraint.
The rest of this article is organized as follows. In Section 2 we collect some properties about the tangent-point potential and introduce our cubic finite element spaces. Section 3 is devoted to a consistency analysis for approximating and discretizing the tangent-point potential and its variation in a periodic setting, i.e., for closed curves. In Section 4 we devise the numerical scheme and discuss its implementation. Numerical experiments are reported in the final Section 5.

2. Preliminaries

II.A. **Sobolev-Slobodeckiĭ spaces.** We consider the torus $\mathbb{R}/\mathbb{Z}$ equipped with the distance $|x|_{\mathbb{R}/\mathbb{Z}} = \inf_{m\in\mathbb{Z}} |x-m|$. The Sobolev space $H^k(\mathbb{R}/\mathbb{Z},\mathbb{R}^3)$ is the closure of the set of all smooth, 1-periodic functions $u:\mathbb{R}\to\mathbb{R}^3$ with respect to the norm

$$\|u\|_{H^k}^2 = \|u\|_{L^2}^2 + \|u^{(k)}\|_{L^2}^2,$$

where the norms on the right-hand side are computed on a fundamental interval, e.g., on $I=[0,1]$. According to [Bla13] (see Lemma II.1 below) curves u with $\mathrm{TP}(u)<\infty$ can be characterized in terms of the Sobolev-Slobodeckiĭ space $W^{2-1/q,q}(\mathbb{R}/\mathbb{Z},\mathbb{R}^3)$ which contains all $u\in H^1(\mathbb{R}/\mathbb{Z},\mathbb{R}^3)$ with $[u']_{W^{1-1/q,q}}<\infty$, where for $s\in(0,1)$ and $p\in[1,\infty)$ we have

$$[f]_{W^{s,p}(\mathbb{R}/\mathbb{Z},\mathbb{R}^3)} = \Big(\iint_{\mathbb{R}/\mathbb{Z}\times\mathbb{R}/\mathbb{Z}} \frac{|f(x)-f(y)|^p}{|x-y|_{\mathbb{R}/\mathbb{Z}}^{1+sp}}\,\mathrm{d}x\,\mathrm{d}y\Big)^{1/p}.$$

The Sobolev-Slobodeckiĭ spaces form a subfamily of Besov spaces and can also be defined via interpolation; see [RS96] for details. We define

$$\|v\|_{W^{s,p}}^p = \|v\|_{L^p}^p + [v]_{W^{s,p}}^p\,.$$

Note that $W^{s,p}(\mathbb{R}/\mathbb{Z},\mathbb{R}^3)$ embeds into $C^{0,s-1/p}(\mathbb{R}/\mathbb{Z},\mathbb{R}^3)$ if $sp>1$. Furthermore, from the embedding $H^1\hookrightarrow W^{s,p}$ for $s-\frac{1}{p}\le\frac{1}{2}$ [RS96], we infer, provided $q\le 4$,

$$\|v\|_{W^{2-1/q,q}} \le C_q\,\|v\|_{H^2} \qquad \text{for any } v\in H^2(\mathbb{R}/\mathbb{Z},\mathbb{R}^3).$$

As we intend to work in H^2 which does not embed into $W^{1+s,p}$ if $s-\frac{1}{p}>\frac{1}{2}$, we will restrict our attention to $q\le 4$.

II.B. **Tangent-point potential.** By $\mathscr{C}_q$ we denote the class of embedded and arc-length parametrized curves $u\in W^{2-1/q,q}(\mathbb{R}/\mathbb{Z},\mathbb{R}^3)$. We quote some known facts about the functional TP.

Lemma II.1 ([Bla13])**.** *Let $q\in(2,\infty)$ and $u\in C^1(\mathbb{R}/\mathbb{Z},\mathbb{R}^3)$ be embedded and parametrized by arc-length. Then the tangent-point energy* TP *takes finite values if and only if $u\in W^{2-1/q,q}$.*

The requirement that u is embedded cannot be omitted, see the discussion in [BR15, Rem. 2.2]. For the case $q = 2$ we refer to [BR15, Rem. 1.6].
The bi-Lipschitz constant $\mathrm{biL}(u)$ of a curve $u \in \mathscr{C}_q$ is defined via

$$\mathrm{biL}(u) = \sup_{x,y\in\mathbb{R}/\mathbb{Z},\, x\neq y} \frac{|x-y|}{|u(x)-u(y)|}$$

and satisfies $\mathrm{biL}(u) \geq 1$. The following lemma provides an upper bound.

Lemma II.2 (Uniform bi-Lipschitz estimate, [BR15, Prop. 2.1])**.** *For any $M < \infty$ and $q \in (2,\infty)$ there is a uniform bound $C_{M,q} < \infty$ on the bi-Lipschitz constant* $\mathrm{biL}(u)$ *for all curves $u \in \mathscr{C}_q$ with* $\mathrm{TP}(u) \leq M$*, so*

$$|x-y|_{\mathbb{R}/\mathbb{Z}} \leq C_{M,q}\,|u(x)-u(y)| \qquad \text{for all } x,y \in \mathbb{R}/\mathbb{Z}.$$

Of course, it is not possible to bound the bi-Lipschitz constant merely in terms of the Sobolev-Slobodeckiĭ norm as the latter does not control self-intersections.
The proof of Lemma II.2 does not extend to the case $q = 2$. However, in this case finite tangent-point energy still implies that the image of the curve is a one-dimensional manifold [SvdM12, Thm. 1.1].
The following statement implies that TP is in fact a *knot energy* if $q > 2$, i.e., it blows up on sequences of embedded curves converging to a curve with a self-intersection. This result has already been obtained in [SSvdM13, Cor. 2.3] by geometric arguments.

Corollary II.3 (Self-avoidance)**.** *Let $(u_k)_{k\in\mathbb{N}} \subset \mathscr{C}_q$ with $q \in (2,\infty)$ pointwise converge to a curve $u_\infty \in C^0(\mathbb{R}/\mathbb{Z},\mathbb{R}^3)$ with a self-intersection, i.e., there are $x,y \in \mathbb{R}/\mathbb{Z}$, $x \neq y$ with $u_\infty(x) = u_\infty(y)$. Then $\mathrm{TP}(u_k) \to \infty$ as $k \to \infty$.*

Proof. Assuming the contrary, we infer from Lemma II.2 the existence of a constant $C < \infty$ with $0 < |x-y|_{\mathbb{R}/\mathbb{Z}} \leq C\,|u_k(x)-u_k(y)|$. As $k \to \infty$ this leads to the contradiction $0 < C\,|u_\infty(x)-u_\infty(y)| = 0$. □

For analytical considerations it is important to note that the integrand in the tangent-point potential can be written as

$$\frac{|u'(y) \wedge (u(x)-u(y))|^q}{|u(x)-u(y)|^{2q}} = \frac{|u'(y) \wedge (u(x)-u(y)-(x-y)u'(y))|^q}{|u(x)-u(y)|^{2q}}. \tag{1}$$

This relation motivates defining the operator

$$(\mathcal{D}v)(x,y) = \frac{v(x)-v(y)-(x-y)v'(y)}{(x-y)^2}. \tag{2}$$

II.C. **Variation of TP.** We next provide a splitting of the variation of TP noting that the functional is differentiable on appropriate classes of curves.

Lemma II.4 ([BR15, Thm. 1.4, Rem. 3.1])**.** *For any $q \in (2,\infty)$ the (parametrization invariant formulation of the) functional* TP *is continuously differentiable on embedded $W^{2-1/q,q}$-curves.*

The statement also holds in the case $q = 2$ if one additionally requires that the curves are continuously differentiable, see [BR15, Rem. 1.6]; recall that $W^{3/2,2}$ does not embed into C^1. The results presented below can in fact be extended to the case $q = 2$, however, to simplify notation, we will restrict our attention to $q > 2$. If $u \in \mathscr{C}_q$ and $\varphi \in W^{2-1/q,q}$, $q \in (2,\infty)$, with $u' \perp \varphi'$, the first variation of TP at u in direction φ simplifies to

$$\delta\mathrm{TP}(u)[\varphi] = \mathcal{M}_0(u;u,\varphi) + \mathcal{M}_0(u;\varphi,u) - 2\mathcal{A}_0(u;u,\varphi)$$

where, for $\varepsilon \in [0,1/2)$ and a set $\mathcal{R}_\varepsilon \subset \mathbb{R}/\mathbb{Z} \times \mathbb{R}/\mathbb{Z}$ with equality for $\varepsilon = 0$, we have

$$\mathcal{M}_\varepsilon(u;v,w) = \iint_{\mathcal{R}_\varepsilon} \frac{|u'(y) \wedge (u(x)-u(y))|^{q-2}}{|u(x)-u(y)|^{2q}} \times \left\langle u'(y) \wedge (u(x)-u(y)), v'(y) \wedge (w(x)-w(y)) \right\rangle \,\mathrm{d}x\,\mathrm{d}y.$$

If $v' \perp w'$ we may replace $w(x)-w(y)$ by $w(x)-w(y)-(x-y)w'(y)$. The mapping $\mathcal{A}_\varepsilon$ is given by

$$\mathcal{A}_\varepsilon(u;v,w) = \iint_{\mathcal{R}_\varepsilon} \frac{|u'(y) \wedge (u(x)-u(y))|^{q}}{|u(x)-u(y)|^{2q+2}} \langle v(x)-v(y), w(x)-w(y)\rangle \,\mathrm{d}x\,\mathrm{d}y.$$

If the integration domain in TP is replaced by $\mathcal{R}_\varepsilon$ we also have for $\varepsilon \in (0,1/2)$

$$\delta\mathrm{TP}_\varepsilon(u)[\varphi] = \mathcal{M}_\varepsilon(u;u,\varphi) + \mathcal{M}_\varepsilon(u;\varphi,u) - 2\mathcal{A}_\varepsilon(u;u,\varphi).$$

II.D. **Approximation spaces.** For the spatial discretization we use conforming subspaces $\mathbb{V}_h \subset H^2(I,\mathbb{R}^\ell)$ that are subordinated to a partition $\mathcal{T}_h$ of I into subintervals I_i of lengths h_i with maximal length h. We identify the partition $\mathcal{T}_h$ with a sequence of nodes $z_1 < z_2 < \cdots < z_{M+1}$ and the space $\mathcal{S}^{1,3}(\mathcal{T}_h,\mathbb{R}^3)$ is given by C^1 splines of piecewise cubic polynomial degree, i.e.,

$$\mathcal{S}^{1,3}(\mathcal{T}_h,\mathbb{R}^3) = \{v_h \in C^1(I,\mathbb{R}^3) : v_h|_{I_i} \in \mathcal{P}_3(I_i)^3,\ i = 1,2,...,M\},$$

where $I_i = [z_i, z_{i+1}]$ and $\mathcal{P}_k(I_i)$ denotes the set of polynomials of degree $k \geq 0$ restricted to I_i. We note that the restriction of $v_h \in \mathcal{S}^{1,3}(\mathcal{T}_h,\mathbb{R}^3)$ to an interval I_i is entirely determined by the values of v_h and v_h' at the endpoints of I_i, i.e., by the four vectors $v_h(z_i)$, $v_h(z_{i+1})$, $v_h'(z_i)$, and $v_h'(z_{i+1})$ that define the positions and tangents of the nodes of the discrete curve. We let

$$\mathcal{L}^0(\mathcal{T}_h \times \mathcal{T}_h) = \left\{v_h \in L^\infty(I\times I) : v_h|_{I_j\times I_k} \text{ constant for } i,j = 1,2,\dots,M\right\}$$

denote the set of piecewise constant functions on the tensor product $\mathcal{T}_h \times \mathcal{T}_h$. Given a set $\mathcal{R} \subset I\times I$ that is the union of rectangles $I_j \times I_k$, $j,k = 1,2,\dots,M$, we define the averaging operator

$$\mathcal{Q}_h : L^\infty(\mathcal{R}) \to \mathcal{L}^0(\mathcal{T}_h \times \mathcal{T}_h)$$

that computes on each rectangle $I_j \times I_k \subset \mathcal{R}$ the average of the values at the four vertices or associates the value 0 otherwise. For any $f \in C^{0,\alpha}(\mathcal{R})$, $\alpha \in (0,1]$, we have

$$\|f - \mathcal{Q}_h f\|_{L^\infty} \leq C h^\alpha [f]_{C^{0,\alpha}}. \tag{3}$$

3. Consistency analysis for closed curves

In this section we provide estimates that control the influences of removing the singular part and using quadrature in the potential TP.

III.A. **Removal of singular part.** For $\varepsilon \in (0,1/2)$ and $u \in \mathscr{C}_q$ we consider

$$\mathrm{TP}_\varepsilon(u) = \tfrac{1}{q} \iint_{\mathcal{R}_\varepsilon} \frac{|u'(y) \wedge (u(x)-u(y))|^q}{|u(x)-u(y)|^{2q}} \,\mathrm{d}x\,\mathrm{d}y,$$

where $\mathcal{R}_\varepsilon$ is any measurable set with

$$\widetilde{\mathcal{R}}_\varepsilon = \big\{(x,y) \in \mathbb{R}/\mathbb{Z} \times \mathbb{R}/\mathbb{Z} : |x-y|_{\mathbb{R}/\mathbb{Z}} \geq \varepsilon\big\} \subset \mathcal{R}_\varepsilon \subset \widetilde{\mathcal{R}}_{\varepsilon/2}.$$

The integrand can be transformed using (1).

Lemma III.1. *We have* $\mathrm{TP}_\varepsilon(u) \nearrow \mathrm{TP}(u)$ *as* $\varepsilon \searrow 0$ *for any* $u \in \mathscr{C}_q$ *and* $q \in [2,\infty)$. *In the case of* $u \in \mathscr{C}_q \cap H^2(\mathbb{R}/\mathbb{Z},\mathbb{R}^3)$ *and* $q \in [2,4)$ *we have*

$$|\mathrm{TP}_\varepsilon(u) - \mathrm{TP}(u)| \leq C_{\delta,q} \varepsilon^{2-q/2-\delta} \,\mathrm{biL}(u)^{2q} \left\|u'\right\|_{H^1}^q$$

for any $\delta \in (0, 2-q/2)$.

Proof. We have $\mathrm{TP}_\varepsilon(u) \leq \mathrm{TP}(u)$ and with $\mathcal{S}_\varepsilon = (\mathbb{R}/\mathbb{Z})^2 \setminus \widetilde{\mathcal{R}}_\varepsilon$

$$\begin{aligned}
q\big(\mathrm{TP}(u) - \mathrm{TP}_\varepsilon(u)\big) &\overset{(1)}{\leq} \iint_{\mathcal{S}_\varepsilon} \frac{|u'(y) \wedge (u(y+z)-u(y)-zu'(y))|^q}{|u(y+z)-u(y)|^{2q}} \,\mathrm{d}z\,\mathrm{d}y \\
&\leq \mathrm{biL}(u)^{2q} \iint_{\mathcal{S}_\varepsilon} \frac{\left|\int_0^1 (u'(y+\vartheta z)-u'(y)) \,\mathrm{d}\vartheta\right|^q}{|z|^q} \,\mathrm{d}z\,\mathrm{d}y \\
&\overset{\text{Jensen}}{\leq} \mathrm{biL}(u)^{2q} \iint_{\mathcal{S}_\varepsilon} \int_0^1 \frac{|u'(y+\vartheta z)-u'(y)|^q}{|z|^q} \,\mathrm{d}\vartheta\,\mathrm{d}z\,\mathrm{d}y \\
&\leq \mathrm{biL}(u)^{2q} \int_0^1 \iint_{\mathcal{S}_{\vartheta\varepsilon}} \vartheta^{q-1} \frac{|u'(y+z)-u'(y)|^q}{|z|^q} \,\mathrm{d}z\,\mathrm{d}y\,\mathrm{d}\vartheta \\
&\leq \mathrm{biL}(u)^{2q} \iint_{\mathcal{S}_\varepsilon} \frac{|u'(y+z)-u'(y)|^q}{|z|^q} \,\mathrm{d}z\,\mathrm{d}y.
\end{aligned}$$

As $u \in W^{2-1/q,q}$, the integrand is in $L^1(\mathbb{R}/\mathbb{Z} \times (-1/2,1/2))$ and the integral vanishes as $\varepsilon \searrow 0$ due to the absolute continuity of the integral. We choose $\delta \in (0, 2-q/2)$ and define $s = 1-\frac{1}{q}$, $\sigma = \frac{1}{2} + \frac{1-\delta}{q}$, $r = \frac{1}{1-\delta}$, $\frac{1}{r} + \frac{1}{r'} = 1$. Using the embedding $H^1 \hookrightarrow W^{\sigma,qr}$ shows

$$\begin{aligned}
&\iint_{\mathcal{S}_\varepsilon} \frac{|u'(y+z)-u'(y)|^q}{|z|^{1+sq}} \,\mathrm{d}z\,\mathrm{d}y \\
&\leq \left[\iint_{\mathcal{S}_\varepsilon} \left(\frac{|u'(y+z)-u'(y)|^q}{|z|^{1/r+\sigma q}}\right)^r \,\mathrm{d}z\,\mathrm{d}y\right]^{1/r} \left[\iint_{\mathcal{S}_\varepsilon} \frac{1}{|z|^{(1-1/r+(s-\sigma)q)r'}} \,\mathrm{d}z\,\mathrm{d}y\right]^{1/r'} \\
&\leq \big[u'\big]_{W^{\sigma,qr}(\mathbb{R}/\mathbb{Z},\mathbb{R}^3)}^q \cdot C_{\delta,q}\varepsilon^{2-q/2-\delta} \leq C_{\delta,q}\varepsilon^{2-q/2-\delta} \left\|u'\right\|_{H^1(\mathbb{R}/\mathbb{Z},\mathbb{R}^3)}^q,
\end{aligned}$$

which implies the estimate. □

Remark III.2. *If $u \in \mathscr{C}_q \cap W^{2,q}(\mathbb{R}/\mathbb{Z},\mathbb{R}^3)$ and $q \in [2,\infty)$ we have*

$$|\mathrm{TP}_\varepsilon(u) - \mathrm{TP}(u)| \le C_q \varepsilon \,\mathrm{biL}(u)^{2q} \left\|u''\right\|^q_{L^q(\mathbb{R}/\mathbb{Z},\mathbb{R}^3)},$$

which follows from the proof of Lemma III.1 with Jensen's inequality, i.e.,

$$\iint_{\mathcal{S}_\varepsilon} \frac{|u'(y+z)-u'(y)|^q}{|z|^q}\,\mathrm{d}z\,\mathrm{d}y \le \iint_{\mathcal{S}_\varepsilon}\int_0^1 \frac{|u''(y+\vartheta z)|^q}{|z|^{q-q}}\,\mathrm{d}\vartheta\,\mathrm{d}z\,\mathrm{d}y \le 2\varepsilon \left\|u''\right\|^q_{L^q}.$$

III.B. **Use of quadrature.** For a partition $\mathcal{T}_h$ of $I=[0,1]$ as in Subsection II.D into subintervals I_j with midpoints x_j, $j=1,2,\dots,M$, we define for $\varepsilon \ge 2h$

$$\mathcal{R}_{\varepsilon,h} = \bigcup_{|x_j-x_k|_{\mathbb{R}/\mathbb{Z}}\ge\varepsilon} I_j \times I_k.$$

Note that if $I_j \times I_k \subset \mathcal{R}_{\varepsilon,h}$ then $\mathrm{dist}_{\mathbb{R}/\mathbb{Z}}(I_j,I_k) \ge \varepsilon/2$. Given $q\in[2,\infty)$ and $u \in C^1(\mathbb{R}/\mathbb{Z},\mathbb{R}^3)$, we introduce the discrete tangent-point energy

$$\mathrm{TP}_{\varepsilon,h}(u) = \tfrac{1}{q}\iint_{\mathcal{R}_{\varepsilon,h}} \mathcal{Q}_h\left[\frac{|u'(y)\wedge(u(x)-u(y))|^q}{|u(x)-u(y)|^{2q}}\right]\mathrm{d}x\,\mathrm{d}y.$$

Proposition III.3. *For any $\varepsilon\in(0,1/2)$, $0<2h\le\varepsilon$, $q\in[2,\infty)$, and $u\in\mathscr{C}_q\cap H^2$ we have*

$$|\mathrm{TP}_{\varepsilon,h}(u) - \mathrm{TP}_\varepsilon(u)| \le C_q\sqrt{h}\left(\frac{\mathrm{biL}(u)}{\varepsilon}\right)^{q+1}\left(\left\|u''\right\|_{L^2}+1\right),$$

where the integration domain of TP_ε is chosen to be $\mathcal{R}_\varepsilon = \mathcal{R}_{\varepsilon,h}$.

Proof. In light of (3) we merely have to show that the function

$$f(x,y) = \frac{|u'(y)\wedge(u(x)-u(y))|^\mu}{|u(x)-u(y)|^\nu}, \qquad \mu = q, \nu = 2q,$$

is $C^{0,1/2}$ on $\mathcal{R}_{\varepsilon,h}$. Note that all factors of f are C^1, except for $u'\in H^1$. Exploiting the embedding $H^1 \hookrightarrow C^{0,1/2}$ on intervals, we infer

$$[f]_{C^{0,1/2}(\mathcal{R}_{\varepsilon,h})} \le \operatorname{ess\,sup}_y \|f(\cdot,y)\|_{H^1(|\cdot-y|\ge\varepsilon/2)} + \operatorname{ess\,sup}_x \|f(x,\cdot)\|_{H^1(|x-\cdot|\ge\varepsilon/2)}.$$

We first note that

$$\|f\|_{L^\infty(\mathcal{R}_{\varepsilon,h})} \le \left\|u'\right\|^\mu_{L^\infty} \sup_{|\xi-\eta|\ge\varepsilon/2}|u(\xi)-u(\eta)|^{\mu-\nu} \le C_{\mu,\nu}\left\|u'\right\|^\mu_{L^\infty}\left(\frac{\mathrm{biL}(u)}{\varepsilon}\right)^{\nu-\mu}.$$

The partial derivatives of f are for $(x,y) \in \mathcal{R}_{\varepsilon,h}$ given by

$$\begin{aligned}
\partial_x f(x,y) &= \mu \frac{|u'(y) \wedge (u(x)-u(y))|^{\mu-2}}{|u(x)-u(y)|^{\nu}} \left\langle u'(y) \wedge (u(x)-u(y)), u'(y) \wedge u'(x) \right\rangle \\
&\quad - \nu \frac{|u'(y) \wedge (u(x)-u(y))|^{\mu}}{|u(x)-u(y)|^{\nu+2}} \left\langle u(x)-u(y), u'(x) \right\rangle, \\
\partial_y f(x,y) &= \mu \frac{|u'(y) \wedge (u(x)-u(y))|^{\mu-2}}{|u(x)-u(y)|^{\nu}} \\
&\quad \times \left\langle u'(y) \wedge (u(x)-u(y)), u''(y) \wedge (u(x)-u(y)) - u'(y) \wedge u'(y) \right\rangle \\
&\quad + \nu \frac{|u'(y) \wedge (u(x)-u(y))|^{\mu}}{|u(x)-u(y)|^{\nu+2}} \left\langle u(x)-u(y), u'(y) \right\rangle.
\end{aligned}$$

We deduce the bounds

$$\begin{aligned}
|\partial_x f| &\le C_{\mu,\nu} \left\|u'\right\|_{L^\infty}^{\mu+1} \sup_{|\xi-\eta| \ge \varepsilon/2} |u(\xi)-u(\eta)|^{\mu-\nu-1} \\
|\partial_y f| &\le C_{\mu,\nu} \left\|u'\right\|_{L^\infty}^{\mu-1} \sup_{|\xi-\eta| \ge \varepsilon/2} |u(\xi)-u(\eta)|^{\mu-\nu} \left|u''(y)\right| \\
&\quad + C_{\mu,\nu} \left\|u'\right\|_{L^\infty}^{\mu+1} \sup_{|\xi-\eta| \ge \varepsilon/2} |u(\xi)-u(\eta)|^{\mu-\nu-1}.
\end{aligned}$$

Recalling $|u'| \equiv 1$, we verify that

$$\begin{aligned}
\|\partial_x f\|_{L^\infty(\mathcal{R}_{\varepsilon,h})} &\le C_{\mu,\nu} \left\|u'\right\|_{L^\infty}^{\mu+1} \left(\frac{\mathrm{biL}(u)}{\varepsilon}\right)^{\nu-\mu+1}, \\
\operatorname{ess\,sup}_x \|\partial_y f(x,\cdot)\|_{L^2(|x-\cdot| \ge \varepsilon)} &\le C_{\mu,\nu} \left\|u'\right\|_{L^\infty}^{\mu+1} \left(\frac{\mathrm{biL}(u)}{\varepsilon}\right)^{\nu-\mu+1} \left(1 + \left\|u''\right\|_{L^2}\right),
\end{aligned}$$

which implies the asserted estimate. □

Remark III.4. *Exploiting the embedding $W^{1-1/q,q} \hookrightarrow C^{0,1-2/q}$, one can alternatively derive an error bound in terms of $h^{1-2/q}$ for $q \in (2,\infty)$. In particular, if $u \in W^{2,q}$ the embedding $W^{1,q} \hookrightarrow C^{0,1-1/q}$ leads to the approximation rate $h^{1-1/q}$. In case that $u \in W^{3,\infty}(\mathbb{R}/\mathbb{Z},\mathbb{R}^3)$ then the identity*

$$f(x,y) = \left| \int_0^1 u'(y+\vartheta(x-y)) \,\mathrm{d}\vartheta \right|^{-2q} \left| u'(y) \wedge \int_0^1 (1-\sigma) u''(y+\sigma(x-y)) \,\mathrm{d}\sigma \right|^{q}$$

where f is defined as in the preceding proof) shows that f is $C^{0,1}$ on $\mathbb{R}/\mathbb{Z} \times \mathbb{R}/\mathbb{Z}$ with a bound depending on the Lipschitz constant of u that is independent of ε. This leads to a linear approximation rate with respect to h. The formula indicates that the integrand f of the tangent point potential is well behaved on the diagonal $x \approx y$. If $u \in W^{4,\infty}$ then we even have $f \in C^{1,1}$ so that a higher order quadrature rule would lead to quadratic convergence in h.

III.C. **Approximation of the variation.** We next derive bounds for the approximation and discretization of the variation of the potential TP.

Lemma III.5. *For $u \in \mathscr{C}_q$, $\varphi \in W^{2-1/q,q}$ with $u' \perp \varphi'$, and $q \in (2,\infty)$ we have $\delta\mathrm{TP}_\varepsilon(u)[\varphi] \to \delta\mathrm{TP}(u)[\varphi]$ as $\varepsilon \searrow 0$. If additionally $u, \varphi \in H^2(\mathbb{R}/\mathbb{Z},\mathbb{R}^3)$ and $q \in (2,4)$ we even arrive at*

$$|\delta\mathrm{TP}_\varepsilon(u)[\varphi] - \delta\mathrm{TP}(u)[\varphi]| \le C_{\delta,q}\varepsilon^{2-q/2-\delta}\,\mathrm{biL}(u)^{2q+2}\,\|u'\|_{H^1}^q\,\|\varphi\|_{H^2}$$

for any $\delta \in (0, 2-q/2)$.

Proof. We proceed as in the proof of Lemma III.1. It is convenient to separately discuss the summands of δTP; using (2) we obtain in case $v' \perp w'$

$$\begin{aligned}
&|\mathcal{M}_\varepsilon(u;v,w) - \mathcal{M}_0(u;v,w)|\\
&\le \iint_{\mathcal{S}_\varepsilon} \big|u'(y) \wedge \mathcal{D}u(x,y)\big|^{q-2}\\
&\qquad\qquad \times \left|\frac{x-y}{u(x)-u(y)}\right|^{2q} \big|u'(y)\wedge\mathcal{D}u(x,y)\big|\,\big|v'(y)\wedge\mathcal{D}w(x,y)\big|\,\mathrm{d}x\,\mathrm{d}y\\
&\le \mathrm{biL}(u)^{2q}\,\|v'\|_{L^\infty}\iint_{\mathcal{S}_\varepsilon} |\mathcal{D}u\,(x,y)|^{q-1}\,|\mathcal{D}w\,(x,y)|\,\mathrm{d}x\,\mathrm{d}y\\
&\le \mathrm{biL}(u)^{2q}\,\|v'\|_{L^\infty}\left[\iint_{\mathcal{S}_\varepsilon} |\mathcal{D}u\,(x,y)|^q\right]^{1-1/q}\left[\iint_{\mathcal{S}_\varepsilon} |\mathcal{D}w\,(x,y)|^q\right]^{1/q}
\end{aligned}$$

and analogously

$$\begin{aligned}
&|\mathcal{A}_\varepsilon(u;v,w) - \mathcal{A}_0(u;v,w)|\\
&\le \iint_{\mathcal{S}_\varepsilon} \frac{|u'(y)\wedge\mathcal{D}u(x,y)|^q}{|u(x)-u(y)|^{2q+2}}|x-y|^{2q}\,|\langle v(x)-v(y),w(x)-w(y)\rangle|\,\mathrm{d}x\,\mathrm{d}y\\
&\le \mathrm{biL}(u)^{2q+2}\iint_{\mathcal{S}_\varepsilon}|\mathcal{D}u(x,y)|^q\left|\frac{v(x)-v(y)}{x-y}\right|\left|\frac{w(x)-w(y)}{x-y}\right|\mathrm{d}x\,\mathrm{d}y\\
&\le \mathrm{biL}(u)^{2q+2}\,\|v'\|_{L^\infty}\,\|w'\|_{L^\infty}\iint_{\mathcal{S}_\varepsilon}|\mathcal{D}u\,(x,y)|^q\,\mathrm{d}x\,\mathrm{d}y.
\end{aligned}$$

Noting that

$$\begin{aligned}
\iint_{\mathcal{S}_\varepsilon}|\mathcal{D}w\,(x,y)|^q\,\mathrm{d}x\,\mathrm{d}y &\le \iint_{\mathcal{S}_\varepsilon}\frac{\left|\int_0^1 (w'(y+\vartheta z)-w'(y))\,\mathrm{d}\vartheta\right|^q}{|z|^q}\,\mathrm{d}z\,\mathrm{d}y\\
&\le \iint_{\mathcal{S}_\varepsilon}\frac{|w'(y+z)-w'(y)|^q}{|z|^q}\,\mathrm{d}z\,\mathrm{d}y,
\end{aligned}$$

the first claim is a consequence of the absolute continuity of the integral. For the second one we argue as in the proof of Lemma III.1. □

For a practical evaluation of δTP we use quadrature and define

$$D\mathrm{TP}_{\varepsilon,h}(u)[\varphi] = \mathcal{M}_{\varepsilon,h}(u;u,\varphi) + \mathcal{M}_{\varepsilon,h}(u;\varphi,u) - 2\mathcal{A}_{\varepsilon,h}(u;u,\varphi),$$

with the mappings $\mathcal{M}_{\varepsilon,h}$ and $\mathcal{A}_{\varepsilon,h}$ defined by

$$\mathcal{M}_{\varepsilon,h}(u;v,w) = \iint_{\mathcal{R}_{\varepsilon,h}} \big\langle (\mathcal{Q}_h\Phi)(x,y), v'(y) \wedge (w(x)-w(y)) \big\rangle \,\mathrm{d}x\,\mathrm{d}y,$$
$$\mathcal{A}_{\varepsilon,h}(u;v,w) = \iint_{\mathcal{R}_{\varepsilon,h}} (\mathcal{Q}_h\Psi)(x,y) \,\langle v(x)-v(y), w(x)-w(y)\rangle \,\mathrm{d}x\,\mathrm{d}y,$$

for functions Φ and Ψ given by

$$\Phi(x,y) = \big|u'(y) \wedge (u(x)-u(y))\big|^{q-2} \frac{u'(y) \wedge (u(x)-u(y))}{|u(x)-u(y)|^{2q}},$$
$$\Psi(x,y) = \frac{|u'(y) \wedge (u(x)-u(y))|^q}{|u(x)-u(y)|^{2q+2}}.$$

Proposition III.6. *For any $\varepsilon \in (0,1/2)$, $0 < 2h \le \varepsilon$, $q \in (2,\infty)$, and $u \in \mathscr{C}_q \cap H^2(\mathbb{R}/\mathbb{Z},\mathbb{R}^3)$ we have for all $\varphi \in H^2(\mathbb{R}/\mathbb{Z},\mathbb{R}^3)$ with $u' \perp \varphi'$ that*

$$\big|\big[D\mathrm{TP}_{\varepsilon,h} - \delta\mathrm{TP}_\varepsilon\big](u)[\varphi]\big| \le C_q\sqrt{h}\left(\frac{\mathrm{biL}(u)}{\varepsilon}\right)^{q+3} \left(\big\|u''\big\|_{L^2}+1\right) \|\varphi\|_{H^2},$$

where the integration domain of TP_ε is chosen to be $\mathcal{R}_\varepsilon = \mathcal{R}_{\varepsilon,h}$.

Proof. As $\delta\mathrm{TP}_\varepsilon$ and $D\mathrm{TP}_{\varepsilon,h}$ are analogously decomposed it is convenient to separately consider the corresponding summands. We obtain, assuming $v' \perp w'$,

$$\big|\big[\mathcal{M}_{\varepsilon,h} - \mathcal{M}_\varepsilon\big](u;v,w)\big| \le \|\Phi - \mathcal{Q}_h\Phi\|_{L^\infty} \iint_{\mathcal{R}_{\varepsilon,h}} \big|v'(y) \wedge (w(x)-w(y))\big| \,\mathrm{d}x\,\mathrm{d}y,$$
$$\big|\big[\mathcal{A}_{\varepsilon,h} - \mathcal{A}_\varepsilon\big](u;v,w)\big| \le \|\Psi - \mathcal{Q}_h\Psi\|_{L^\infty} \iint_{\mathcal{R}_{\varepsilon,h}} \big|v'(y) \wedge (w(x)-w(y))\big| \,\mathrm{d}x\,\mathrm{d}y.$$

Noting estimate (3) with $\alpha = 1/2$ we deduce that

$$|\mathcal{M}_{\varepsilon,h}(u;v,w) - \mathcal{M}_\varepsilon(u;v,w)| \le C\sqrt{h}\,[\Phi]_{C^{0,1/2}(\mathcal{R}_{\varepsilon,h})} \big\|v'\big\|_{L^\infty} \big\|w'\big\|_{L^\infty},$$
$$|\mathcal{A}_{\varepsilon,h}(u;v,w) - \mathcal{A}_\varepsilon(u;v,w)| \le C\sqrt{h}\,[\Psi]_{C^{0,1/2}(\mathcal{R}_{\varepsilon,h})} \big\|v'\big\|_{L^\infty} \big\|w'\big\|_{L^\infty}.$$

The argument in the proof of Proposition III.3 extends to arbitrary positive reals $\mu < \nu$, so letting $(\mu,\nu) = (q-1,2q)$ and $(\mu,\nu) = (q,2q+2)$ yields the desired bound. □

Analogously to Remark III.4, an inspection of the proof shows that the additional assumption $u,\varphi \in W^{2,q}(\mathbb{R}/\mathbb{Z},\mathbb{R}^3)$ yields an approximation rate in terms of $h^{1-1/q}$ while $u,\varphi \in W^{3,\infty}(\mathbb{R}/\mathbb{Z},\mathbb{R}^3)$ leads to a linear approximation rate with respect to h.

4. Numerical scheme

IV.A. **Discrete gradient flow.** As a model problem and application of our consistency estimates we consider the approximation of a family of arc-length parametrized curves $u(t,\cdot) : I \to \mathbb{R}^3$ for $t \in [0,T]$ such that

$$(\partial_t u, w) = -\delta\big(I_{\mathrm{bend}} + \varrho \mathrm{TP}_\varepsilon\big)(u)[w]$$

for all $w : I \to \mathbb{R}^3$ satisfying $u'(t,\cdot)\cdot w = 0$ in I. With the decomposition of $\delta\mathrm{TP}_\varepsilon$ introduced above, the evolution problem reads

$$(\partial_t u, w) = -\mathcal{B}(u,w) - 2\varrho\mathcal{M}_\varepsilon^{\mathrm{sym}}(u;u,w) + 2\varrho\mathcal{A}_\varepsilon(u;u,w),$$

where $(\cdot,\cdot)$ denotes the L^2 scalar product,

$$2\mathcal{M}_\varepsilon^{\mathrm{sym}}(u;v,w) = \mathcal{M}_\varepsilon(u;v,w) + \mathcal{M}_\varepsilon(u;w,v).$$

and the bilinear form $\mathcal{B}$ is the variation of the bending energy

$$\mathcal{B}(v,w) = (v'',w'').$$

We consider here an interval $I \subset \mathbb{R}$ and include homogeneous or periodic boundary conditions in the discrete linear space

$$\mathbb{V}_h \subset \mathcal{S}^{1,3}(\mathcal{T}_h,\mathbb{R}^3).$$

Inhomogeneous boundary conditions will be included via the initial curve u^0. Given some $u_h \in \mathcal{S}^{1,3}(\mathcal{T}_h,\mathbb{R}^3)$ we include the linearized arc-length condition in the space

$$\mathbb{F}_h[u_h] = \big\{v_h \in \mathbb{V}_h : v_h'(z_i)\cdot u_h'(z_i) = 0 \text{ for } i = 1,2,\dots,M+1\big\}.$$

Our numerical scheme realizes a semi-implicit treatment of the evolution problem with a linearized treatment of the constraint.

Algorithm IV.1 (Semi-implicit time-stepping)**.** *Let $\mathcal{T}_h$ be a partioning of I, let $u_h^0 \in \mathcal{S}^{1,3}(\mathcal{T}_h,\mathbb{R}^3)$ with $|[u_h^0]'(z_i)|^2 = 1$ for $i = 1,\dots,M+1$, and let $\varepsilon,\tau > 0$. Set $n = 1$.*
(1) Compute $v_h^n \in \mathbb{F}_h[u_h^{n-1}]$ such that

$$\begin{aligned}(v_h^n,w_h) + \tau\mathcal{B}(v_h^n,w_h) + 2\varrho\tau\mathcal{M}_{\varepsilon,h}^{\mathrm{sym}}(u_h^{n-1};v_h^n,w_h)\\ = -\mathcal{B}(u_h^{n-1},w_h) - 2\varrho\mathcal{M}_{\varepsilon,h}^{\mathrm{sym}}(u_h^{n-1};u_h^{n-1},w_h) + 2\varrho\mathcal{A}_{\varepsilon,h}(u_h^{n-1};u_h^{n-1},w_h)\end{aligned}$$

for all $w_h \in \mathbb{F}_h[u_h^{n-1}]$.
(2) Set $u_h^n = u_h^{n-1} + \tau v_h^n$. Stop if $n\tau \geq T$; increase $n \to n+1$ and continue with (1) otherwise.

The motivation for the particular semi-implicit treatment of the variation of the potential is the fact that $\mathcal{A}_\varepsilon(u;\cdot,\cdot)$ is a positive semi-definite bilinear form while $\mathcal{M}_\varepsilon(u;\cdot,\cdot)$ is non-negative in a neighborhood of (u,u).

IV.B. **Discrete energy barrier.** To limit the influence of the self-avoidance potential on the evolution but to still enforce embededness of curves, we aim at determining a suitable parameter $\varrho = h^\alpha$ in terms of the mesh-size $h > 0$. Our discretization of TP leads to the identity

$$\mathrm{TP}_{\varepsilon,h}(u_h) = \frac{1}{q} \sum_{\substack{i,j=1,\dots,M+1 \\ |z_i - z_j| > \varepsilon}} h_i h_j \gamma_i \gamma_j \frac{|u_h'(z_i) \wedge [u_h(z_i) - u_h(z_j)]|^q}{|u_h(z_i) - u_h(z_j)|^{2q}}$$

with certain weights γ_i that are independent of the mesh-size. A discrete self-intersection corresponds to a configuration of non-neighboring nodes z and $\widetilde{z}$ such that

$$|u_h(z) - u_h(\widetilde{z})| \sim h$$

and if $u_h'(z)$ and $u_h(z) - u_h(\widetilde{z})$ are non-tangential we have

$$\mathrm{TP}_{\varepsilon,h}(u_h) \geq c h^{2-q},$$

cf. Fig. 2. This shows that $q = 2$ may be insufficient to avoid self-intersections. To introduce a discrete energy barrier we thus have to choose

$$\varrho \geq c h^{q-2-\sigma}$$

for some $\sigma > 0$.

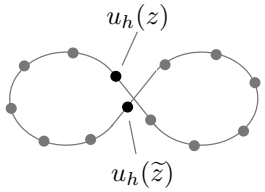

FIGURE 2. Self-intersection of a planar curve not detected by the discretized potential if $q = 2$ (black dots indicate images of nodes z and $\widetilde{z}$).

The parameter ϱ introduces a length scale in the mathematical model that determines how close a curve may be to itself.

IV.C. **Assembly.** We discuss here the numerical computation of terms resulting from the differentiation and discretization of the tangent point energy. We set $n_E = M$ and for a partition $I = \cup_{j=1}^{n_E} I_j$ into closed intervals I_j of lengths h_j and with midpoints x_j, $j = 1, 2, \dots, n_E$, we note

$$\mathrm{TP}_{\varepsilon,h}(u_h) = \int_{\mathcal{R}_{\varepsilon,h}} \mathcal{Q}_h \lambda_h(x,y)\,\mathrm{d}x\,\mathrm{d}y = \sum_{\substack{j,k=1,\dots,n_E \\ |x_j - x_k| \geq \varepsilon}} \mathcal{Q}_h \lambda_h|_{I_j \times I_k} h_j h_k,$$

where

$$\lambda_h(x,y) = \frac{1}{q} \frac{|u_h'(y) \wedge [u_h(y) - u_h(x)]|^q}{|u_h(y) - u_h(x)|^{2q}}.$$

The operator $\mathcal{Q}_h$ computes on each rectangle $I_j \times I_k$ the constant value obtained as the average of the values at the vertices. Similarly, we have

$$\begin{aligned}\mathcal{A}_{\varepsilon,h}(u_h;v_h,w_h) &= \int_{\mathcal{R}_{\varepsilon,h}} (\mathcal{Q}_h\Psi_h)(x,y)\ \langle v_h(y)-v_h(x), w_h(y)-w_h(x)\rangle\ \mathrm{d}x\,\mathrm{d}y\\ &= \sum_{\substack{j,k=1,\dots,n_E\\ |x_j-x_k|\geq\varepsilon}} \mathcal{Q}_h\Psi_h|_{I_j\times I_k} \int_{I_j\times I_k} \langle v_h(y)-v_h(x), w_h(y)-w_h(x)\rangle\ \mathrm{d}x\,\mathrm{d}y,\end{aligned}$$

where

$$\Psi_h(x,y) = \frac{|u_h'(y)\wedge(u_h(y)-u_h(x))|^q}{|u_h(y)-u_h(x)|^{2q+2}},$$

and

$$\begin{aligned}\mathcal{M}_{\varepsilon,h}(u_h;v_h,w_h) &= \int_{\mathcal{R}_{\varepsilon,h}} (\mathcal{Q}_h\Phi_h)(x,y)\cdot\big[v_h'(y)\wedge\big(w_h(y)-w_h(x)\big)\big]\,\mathrm{d}x\,\mathrm{d}y\\ &= \sum_{\substack{j,k=1,\dots,n_E\\ |x_j-x_k|\geq\varepsilon}} \mathcal{Q}_h\Phi_h|_{I_j\times I_k}\cdot\int_{I_j\times I_k} v_h'(y)\wedge\big(w_h(y)-w_h(x)\big)\,\mathrm{d}x\,\mathrm{d}y,\end{aligned}$$

where

$$\Phi_h(x,y) = \frac{|u_h'(y)\wedge[u_h(y)-u_h(x)]|^{q-2}\,u_h'(y)\wedge\big(u_h(y)-u_h(x)\big)}{|u_h(y)-u_h(x)|^{2q}}.$$

The functions u_h, v_h, w_h are linear combinations of basis functions $\varphi_m e_p$, $m=1,2,\dots,2n_C$, $p=1,2,3$, associated with the nodes $z_1,z_2,\dots,z_{n_C}$ with $n_C = M+1$ of the partition and the canonical basis vectors $e_p\in\mathbb{R}^3$, $p=1,2,3$. In particular, to a node z_ℓ two basis functions $\varphi_{2\ell-1}$ and $\varphi_{2\ell}$ are associated which are defined by the conditions

$$\varphi_{2\ell-1}(z_i)=\delta_{\ell i},\quad \varphi_{2\ell-1}'(z_i)=0,$$

and

$$\varphi_{2\ell}(z_i)=0,\quad \varphi_{2\ell}'(z_i)=\delta_{\ell i},$$

for $i=1,2,\dots,n_C$. Note that odd and even basis functions have to be scaled differently when transformed from a reference element, e.g.,

$$\varphi_m|_{I_j} = h_j^{m \bmod 2+1}\widetilde{\varphi}_{m'}\circ\Phi_j$$

with affine transformation $\Phi_j : I_j\to[0,1]$. In particular, contributions to the bilinear form are computed via

$$\int_{I_j}\varphi_m^{(\alpha)}\varphi_n^{(\beta)}\,\mathrm{d}x = h_j^{1-\alpha-\beta}h_j^{m \bmod 2+1}h_j^{n \bmod 2+1}\int_0^1\widetilde{\varphi}_{m'}^{(\alpha)}\widetilde{\varphi}_{n'}^{(\beta)}\,\mathrm{d}\widetilde{x}.$$

For the assembly of $\mathcal{A}_{\varepsilon,h}$ we define $v_h^q = v_h\cdot e_q$ and note that every basis function φ_n is supported on at most two neighboring intervals and that I_j

and I_k are nonneighboring provided that $\varepsilon \geq 2h$. Hence, we have

$$\begin{aligned}
&\mathcal{A}_{\varepsilon,h}(u_h; v_h, \varphi_n e_q) \\
&= \sum_{\substack{j,k=1,\dots,n_E \\ |x_j - x_k| \geq \varepsilon}} \mathcal{Q}_h \Psi_h|_{I_j \times I_k} \int_{I_j \times I_k} \big(v_h^q(y) - v_h^q(x)\big)\big(\varphi_n(y) - \varphi_n(x)\big)\,\mathrm{d}x\,\mathrm{d}y \\
&= \sum_{\substack{j,k=1,\dots,n_E \\ |x_j - x_k| \geq \varepsilon}} \mathcal{Q}_h \Psi_h|_{I_j \times I_k} \cdot \begin{cases} |I_j| \int_{I_k} v_h^q \varphi_n \,\mathrm{d}y - \int_{I_j} v_h^q \,\mathrm{d}x \int_{I_k} \varphi_n \,\mathrm{d}y & \text{if } z^{[n]} \in I_k, \\ |I_k| \int_{I_j} v_h^q \varphi_n \,\mathrm{d}x - \int_{I_j} \varphi_n \,\mathrm{d}x \int_{I_k} v_h^q \,\mathrm{d}y & \text{if } z^{[n]} \in I_j, \\ 0 & \text{otherwise,} \end{cases}
\end{aligned}$$

where $z^{[n]}$ is the node associated with the basis function φ_n. Terms defined by $\mathcal{M}_{\varepsilon,h}$ are treated implicitly and we compute

$$\begin{aligned}
&\mathcal{M}_{\varepsilon,h}(u_h; \varphi_m e_p, \varphi_n e_q) \\
&= \sum_{\substack{j,k=1,\dots,n_E \\ |x_j - x_k| \geq \varepsilon}} \mathcal{Q}_h \Phi_h|_{I_j \times I_k} \cdot (e_p \wedge e_q) \int_{I_j \times I_k} \varphi_m'(y)\big(\varphi_n(y) - \varphi_n(x)\big)\,\mathrm{d}x\,\mathrm{d}y \\
&= \sum_{\substack{j,k=1,\dots,n_E \\ |x_j - x_k| \geq \varepsilon}} \mathcal{Q}_h \Phi_h|_{I_j \times I_k} \cdot (e_p \wedge e_q) \cdot \begin{cases} |I_j| \int_{I_k} \varphi_m' \varphi_n \,\mathrm{d}y & \text{if } z^{[m]}, z^{[n]} \in I_k, \\ -\int_{I_j} \varphi_n \,\mathrm{d}x \int_{I_k} \varphi_m' \,\mathrm{d}y & \text{if } \big(z^{[m]}, z^{[n]}\big) \in I_k \times I_j, \\ 0 & \text{otherwise.} \end{cases}
\end{aligned}$$

Note that in a periodic setting the nodes z_1 and z_{M+1} are identified and sums are over pairs of indices (j,k) with $|x_j - x_k|_{\mathbb{R}/\mathbb{Z}} \geq \varepsilon$.

5. Numerical experiments

In this section we report on experiments which verify the consistency estimates and discrete evolutions computed with the numerical scheme described in Algorithm IV.1 to illustrate its practical stability properties and the underlying evolution process. Throughout we assume that the flow provides sufficient regularity so that the approximation rates derived under additional regularity assumpations are valid.

V.A. Experimental convergence rates.

We consider a smooth planar closed curve and verify the experimental convergence rate of $\mathrm{TP}_{\varepsilon,h}$ as the approximation paramers (h,ε) tend to 0.

Example V.1. *We let* $I = [0, 2\pi]$ *and*

$$u(y) = \begin{bmatrix} \cos(y) \\ \sin(y) \\ 0 \end{bmatrix}.$$

With standard trigonometrical identities and asymmetry of sin *we find that*

$$q\mathrm{TP}(u) = \iint_{I \times I} \frac{\big(\cos(y)(\cos(y) - \cos(x)) + \sin(y)(\sin(y) - \sin(x))\big)^q}{\big((\cos(y) - \cos(x))^2 + (\sin(y) - \sin(x))^2\big)^q}\,\mathrm{d}x\,\mathrm{d}y.$$

We thus have that $\mathrm{TP}(u) = 2^{2-q}\pi^2/q$. *For the summands in the decomposition of the variation of* TP *we have* $\mathcal{M}_0(u;u,u) = q\mathrm{TP}(u)$ *and* $\mathcal{A}_0(u;u,u) = q\mathrm{TP}(u)$.

Table 1 shows for a sequence of uniform partitions of I with meshsizes $h_j = 2^{-j}/10$, $j = 0, 1, \dots, 5$ the relative errors

$$\begin{aligned}
\delta^h_{\mathrm{TP}} &= \big|\mathrm{TP}_{\varepsilon,h}(I_h u) - \mathrm{TP}(u)\big|/\mathrm{TP}(u),\\
\delta^h_{\mathcal{M}} &= \big|\mathcal{M}_{\varepsilon,h}(I_h u; I_h u, I_h u) - \mathcal{M}(u;u,u)\big|/\mathcal{M}(u;u,u),\\
\delta^h_{\mathcal{A}} &= \big|\mathcal{A}_{\varepsilon,h}(I_h u; I_h u, I_h u) - \mathcal{A}(u;u,u)\big|/\mathcal{A}(u;u,u).
\end{aligned}$$

For our experiment we chose the parameters

$$q = 3, \quad \varepsilon = 2h.$$

Note that our error analysis considers the case $\mathcal{M}(u;v,w)$ with $v' \perp w'$. We observe a nearly linear rate of convergence for all errors. The error quantities $\delta^j_{\mathcal{M}}$ and $\delta^j_{\mathcal{A}}$ coincide for the particular choice of functions.

h_j	δ^j_{TP}	$\delta^j_{\mathcal{M}}$	$\delta^j_{\mathcal{A}}$
$2^{-0}/10$	0.103 814	0.084 572	0.084 572
$2^{-1}/10$	0.049 860	0.039 296	0.039 296
$2^{-2}/10$	0.022 408	0.016 876	0.016 876
$2^{-3}/10$	0.012 522	0.009 712	0.009 712
$2^{-4}/10$	0.005 584	0.004 163	0.004 163
$2^{-5}/10$	0.003 100	0.002 387	0.002 387

TABLE 1. Approximation errors in Example V.1 for a smooth curve and different mesh sizes. A nearly linear experimental order of convergence is observed.

τ	$\varrho = 1$	$\varrho = h^{1/2}$	$\varrho = 0.01 \cdot h^{1/2}$
1	N	Y	Y
h	Y	Y	Y
$h/4$	Y	Y	Y

TABLE 2. Experimental stability analysis for Algorithm IV.1 with fixed mesh-size $h \sim 1/80$ in Example V.2. An entry Y indicates that the total energy I^{tot}_h remained bounded by its initial value whereas N refers to an instability.

V.B. **Evolution of a trefoil knot.** We consider a periodic setting and as initial curve a trefoil knot to study the evolution defined by the discrete gradient flow.

Example V.2. *For $T = 200$ and $\widetilde{I} = [0,1]$ let*

$$\widetilde{u}(\widetilde{y}) = \begin{bmatrix} (2+\cos(6\pi\widetilde{y}))\cos(4\pi\widetilde{y}) \\ (2+\cos(6\pi\widetilde{y}))\sin(4\pi\widetilde{y}) \\ \sin(6\pi\widetilde{y}) \end{bmatrix}.$$

Via a reparametrization $\phi : \widetilde{I} \to I = [0, L]$ with the length L of the curve $\widetilde{u}$ we obtain an arc-length parametrized mapping $u : I \to \mathbb{R}^3$ that describes the same curve.

For partitions $\mathcal{T}_h$ of I with $h \sim 1/M$ we set

$$q = 3, \quad \tau = h/4, \quad \varepsilon = 2h, \quad \varrho = h^{1/2}/100.$$

Figure 5 shows for different mesh-sizes the values of the total weighted energy and the potential

$$I_h^{\mathrm{tot}}(u_h^n) = I_{\mathrm{bend}}(u_h^n) + \varrho \mathrm{TP}_{\varepsilon,h}(u_h^n), \quad \mathrm{TP}_{\varepsilon,h}(u_h^n),$$

as functions of $t_n = n\tau$, $n = 0, 1, \ldots, N$, for $N \approx T/\tau$. We see that the discrete energy $I_h^{\mathrm{tot}}(u_h^n)$ is monotonically decreasing indicating good stability properties of our numerical scheme. Except for the case $M = 20$ we see that the potential increases and reaches a barrier value that prevents the curve from undergoing a topological change. This effect is also apparent from Figure 3, in which we plotted snapshots of the discrete evolution for the mesh-size $h = 1/40$. We see that the curve immediately relaxes its bending energy and attains a constant state. Final states for different mesh-sizes are shown in Figure 4 which are stationary configurations for $h \sim 1/40$ and $h \sim 1/80$. The weighting factor ϱ is too small in case $h \sim 1/20$ to guarantee self-avoidance and the evolution is towards a simple circle. Due to the decreasing factor in front of the potential we observe that the minimal distance up to which the curve may come close to itself decreases with the mesh-size. The geometry of constant states as $\varrho \searrow 0$ are discussed in [GRvdM15] where instead of TP a non-smooth self-avoiding functional is considered.

To understand the stability properties of the iteration of Algorithm IV.1 we tried for fixed $M = 80$ the weighting parameters

$$\varrho = 1,\ h^{1/2}, h^{1/2}/100,$$

and step sizes

$$\tau = 1,\ h,\ h/4.$$

Table 2 indicates whether the total energy I_h^{tot} remained bounded during the discrete evolution. We observe that only for $\varrho = \tau = 1$ an instability occurs. In all other settings the evolution attains a stationary state that is comparable to those shown in the second and third plot of Figure 4. The experiment thus indicates stability provided that $\tau\varrho \leq h^{1/2}$. In particular, no self-intersections occur for this relation.

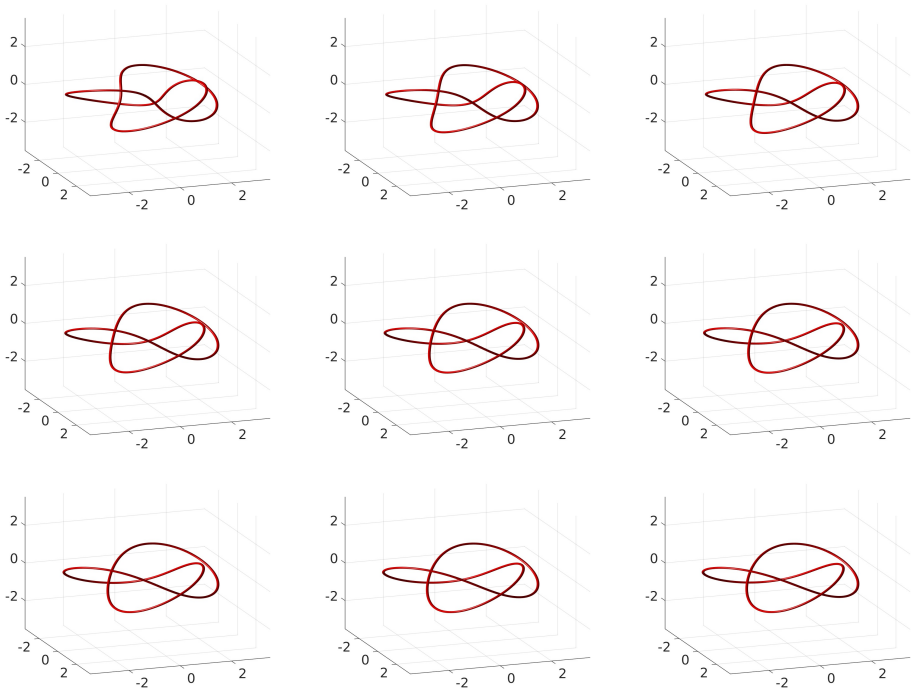

FIGURE 3. Snapshots u_h^n, $n = 0, 1, \dots, 8$, of the initial discrete evolution defined by Example V.2 for mesh-size $h \sim 1/40$. The curve relaxes bending energy but its evolution is stopped by the potential before the curve self-intersects.

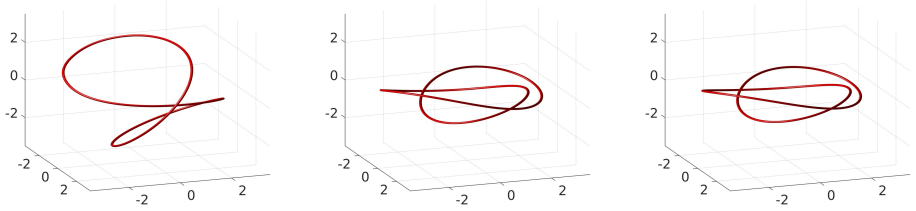

FIGURE 4. Discrete configurations at $T = 200$ for mesh-sizes $h \sim 1/20$, $1/40$, $1/80$ in Example V.2. The choice $\varrho = h^{1/2}/100$ is too small to avoid self-penetration for $h \sim 1/20$. For $h \sim 1/40$, $1/80$ the curves remain embedded throughout the discrete evolution and attain a stationary configuration which becomes flatter as $h \to 0$ due to the weighting of the potential.

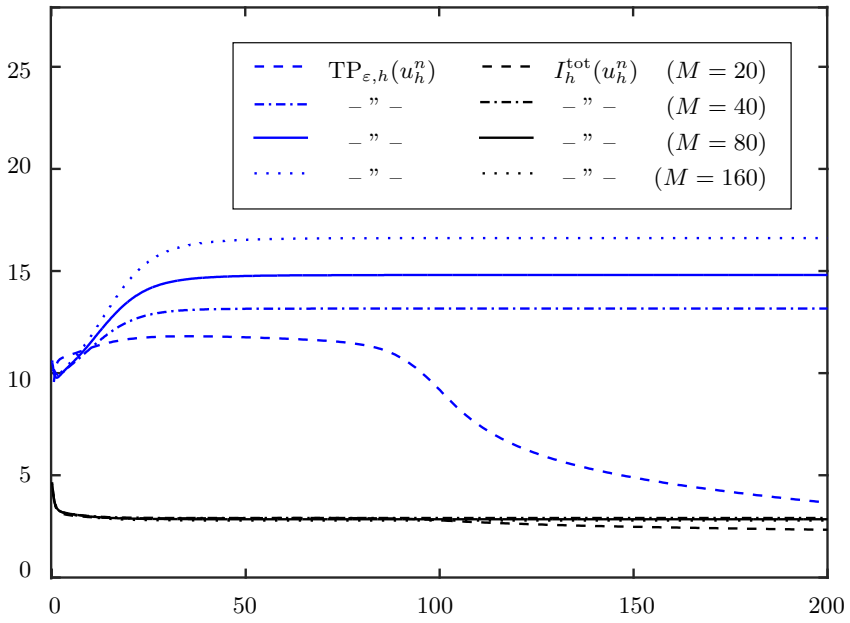

FIGURE 5. Discrete total weighted energy I_h^{tot} and potential $\mathrm{TP}_{\varepsilon,h}$ as functions of u_h^n, $n = 0, 1, \ldots, N$, versus $t_n = n\tau \in [0, 200]$ for the discrete evolution defined by Example V.2 with different mesh-sizes $h \sim 1/M$.

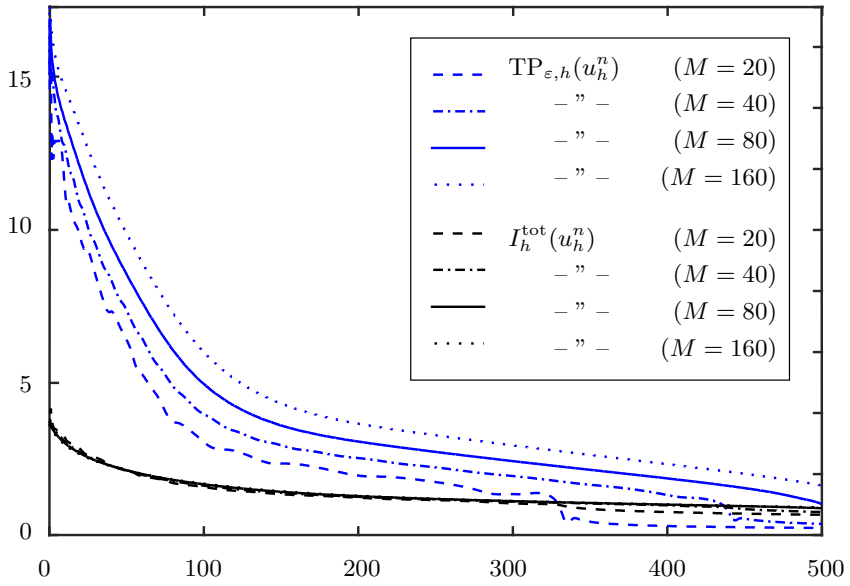

FIGURE 6. Discrete total weighted energy I_h^{tot} and potential $\mathrm{TP}_{\varepsilon,h}$ as functions of u_h^n, $n = 0, 1, \ldots, N$, versus $t_n = n\tau \in [0, 500]$ for the discrete evolution defined by Example V.3 with different mesh-sizes $h \sim 1/M$.

V.C. **Unwinding of a clamped spiral.** Our third experiment considers a planar spiral curve that is clamped at its outer and free at its inner end.

Example V.3. *Let* $T = 500$ $\widetilde{I} = [0,1]$ *and*

$$u(\widetilde{y}) = \begin{bmatrix} 20\cos(2\pi(2\widetilde{y}+1))/(2\pi(2\widetilde{y}+1)) \\ 20\sin(2\pi(2\widetilde{y}+1))/(2\pi(2\widetilde{y}+1)) \\ 0 \end{bmatrix}.$$

Via a reparametrization $\phi : \widetilde{I} \to I = [0, L]$ *with the length* L *of the curve* $\widetilde{u}$ *we obtain an arc-length parametrized mapping* $u : I \to \mathbb{R}^3$ *that describes the same curve.*

We again consider a sequence of partitions $\mathcal{T}_h$ of I with maximal mesh-sizes $h \sim 1/M$, that result from a transformation of a uniform partition of $\widetilde{I} = [0,1]$, and associated parameters

$$q = 3, \quad \tau = h/4, \quad \varepsilon = 2h, \quad \varrho = h^{1/2}/100.$$

The good stability properties of our numerical scheme are again confirmed by Figure 5 where we plotted the values of the total weighted energy and the potential

$$I_h^{\mathrm{tot}}(u_h^n) = I_{\mathrm{bend}}(u_h^n) + \varrho \mathrm{TP}_{\varepsilon,h}(u_h^n), \quad \mathrm{TP}_{\varepsilon,h}(u_h^n),$$

as functions of $t_n = n\tau$, $n = 0, 1, \ldots, N$, for $N \approx T/\tau$. Opposed to the experiments of the previous section the potential does not attain a constant mesh-size dependent value but decays to zero. This is due to the fact that the curve can entirely relax to a straight line without undergoing self-intersections. Snapshots of the discrete evolution for the mesh-size $h \sim 1/40$ are displayed in Figure 7 which illustrate this behavior. The discrete states at time $T = 500$ shown in Figure 8 reveal a slight mesh-dependence of the speed of the evolution which is related to the mesh dependence of the weighting factor ϱ in the energy functional that defines the evolution.

References

[Bar13] Sören Bartels, *A simple scheme for the approximation of the elastic flow of inextensible curves*, IMA J. Numer. Anal. **33** (2013), no. 4, 1115–1125.

[BGN12] John W. Barrett, Harald Garcke, and Robert Nürnberg, *Parametric approximation of isotropic and anisotropic elastic flow for closed and open curves*, Numer. Math. **120** (2012), no. 3, 489–542.

[Bla13] Simon Blatt, *The energy spaces of the tangent point energies*, J. Topol. Anal. **5** (2013), no. 3, 261–270.

[BR15] Simon Blatt and Philipp Reiter, *Regularity theory for tangent-point energies: the non-degenerate sub-critical case*, Adv. Calc. Var. **8** (2015), no. 2, 93–116.

[DKS02] Gerhard Dziuk, Ernst Kuwert, and Reiner Schätzle, *Evolution of elastic curves in* $\mathbb{R}^n$*: existence and computation*, SIAM J. Math. Anal. **33** (2002), no. 5, 1228–1245.

[DLP14] Anna Dall'Acqua, Chun-Chi Lin, and Paola Pozzi, *Evolution of open elastic curves in* $\mathbb{R}^n$ *subject to fixed length and natural boundary conditions*, Analysis (Berlin) **34** (2014), no. 2, 209–222.

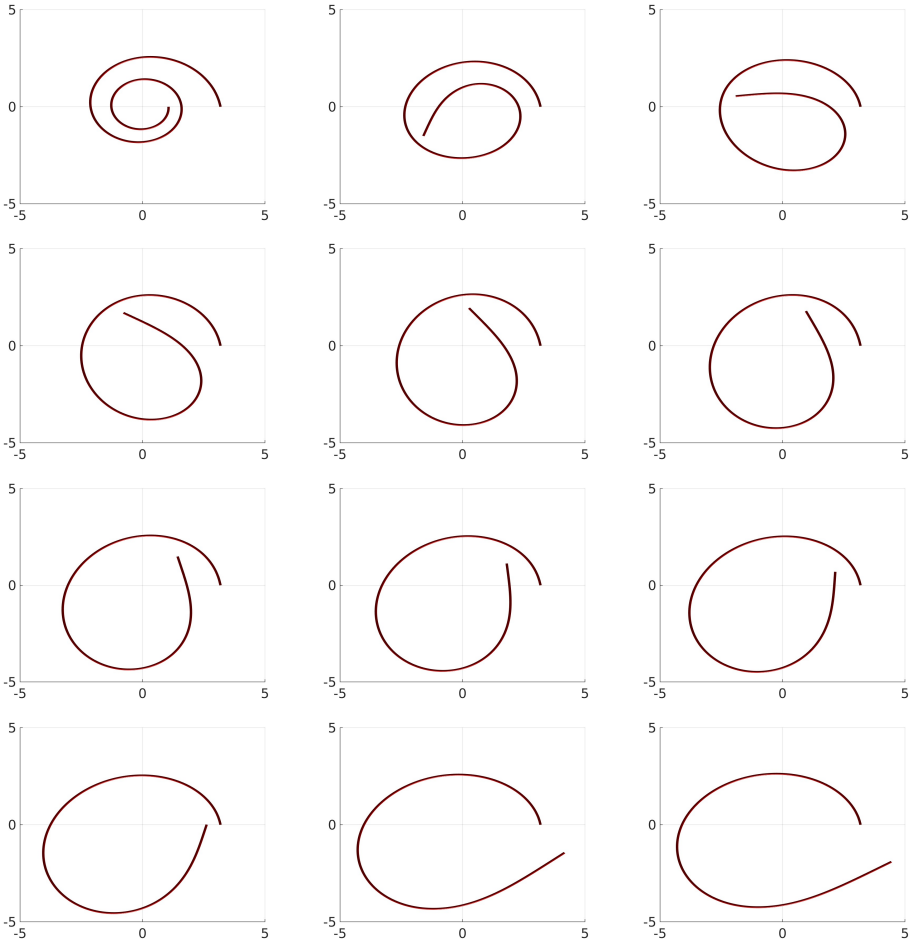

FIGURE 7. Snapshots of the discrete evolution defined by Example V.3 for mesh-size $h \sim 1/40$ after $j \cdot 200$, $j = 0, \ldots, 11$, steps. The clamped curve relaxes its bending energy and tends to form a straight line.

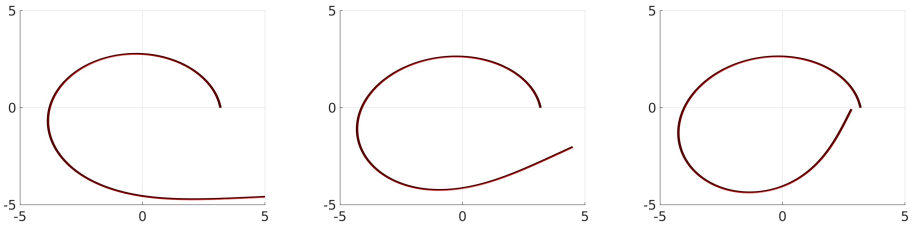

FIGURE 8. Discrete configurations at $T = 500$ for mesh-sizes $h \sim 1/20, 1/40, 1/80$ in Example V.3. The speed of evolution is slightly decreased as $h \to 0$.

[GM99] Oscar Gonzalez and John H. Maddocks, *Global curvature, thickness, and the ideal shapes of knots*, Proc. Natl. Acad. Sci. USA **96** (1999), 4769–4773.

[GM15] Martin Grothaus and Nicole Marheineke, *On a nonlinear partial differential algebraic system arising in the technical textile industry: analysis and numerics*, IMA Journal of Numerical Analysis (2015).

[GRvdM15] Henryk Gerlach, Philipp Reiter, and Heiko von der Mosel, *The elastic trefoil is the twice covered circle*, ArXiv e-prints (2015).

[Her12] Tobias Hermes, *Analysis of the first variation and a numerical gradient flow for integral Menger curvature*, Ph.D. thesis, RWTH Aachen University, 2012, http://publications.rwth-aachen.de/record/82904.

[MM03] Maria Giovanna Mora and Stefan Müller, *Derivation of the nonlinear bending-torsion theory for inextensible rods by* Γ*-convergence*, Calc. Var. Partial Differential Equations **18** (2003), no. 3, 287–305.

[MOSS15] Angelika Manhart, Dietmar Oelz, Christian Schmeiser, and Nikolaos Sfakianakis, *An extended filament based lamellipodium model produces various moving cell shapes in the presence of chemotactic signals*, J. Theoret. Biol. **382** (2015), 244–258.

[PS15] Paola Pozzi and Björn Stinner, *Curve shortening flow coupled to lateral diffusion*, ArXiv e-prints (2015), no. 1510.06173.

[RS96] Thomas Runst and Winfried Sickel, *Sobolev spaces of fractional order, Nemytskij operators, and nonlinear partial differential equations*, de Gruyter Series in Nonlinear Analysis and Applications, vol. 3, Walter de Gruyter & Co., Berlin, 1996.

[Sch16] Sebastian Scholtes, *Discrete knot energies*, ArXiv e-prints (2016).

[SSvdM13] Pawel Strzelecki, Marta Szumańska, and Heiko von der Mosel, *On some knot energies involving Menger curvature*, Topology Appl. **160** (2013), no. 13, 1507–1529. MR 3091327

[SvdM12] Pawel Strzelecki and Heiko von der Mosel, *Tangent-point self-avoidance energies for curves*, J. Knot Theory Ramifications **21** (2012), no. 5, 1250044, 28.

[Wal16] Shawn W. Walker, *Shape optimization of self-avoiding curves*, J. Comput. Phys. **311** (2016), 275–298.

Abteilung für Angewandte Mathematik, Albert-Ludwigs-Universität Freiburg, Hermann-Herder Str. 10, 79104 Freiburg i.Br., Germany

Fakultät für Mathematik, Universität Duisburg-Essen, 45117 Essen, Germany

Abteilung für Angewandte Mathematik, Albert-Ludwigs-Universität Freiburg, Hermann-Herder Str. 10, 79104 Freiburg i.Br., Germany